

The power spectrum indicator: A new, efficient method for the early detection of chaos.

Ch Vozikis¹, K Kleidis² and S Papaioannou¹

¹ Department of Civil Engineering and Surveying & Geoinformatics Engineering, Technological Education Institute of Central Macedonia, 621.24 Serres, Greece

² Department of Mechanical Engineering, Technological Education Institute of Central Macedonia, 621.24 Serres, Greece

E-mail: chriss@teicm.gr, kleidis@teicm.gr and pasta@teicm.gr

Abstract. To determine the regular or chaotic nature of the orbits in dynamical systems can be quite an issue. In this article, following Vozikis et al. (2000), we propose a new tool, namely, the Power Spectrum Indicator (PSI), ψ^2 , that enables us to determine, as early as possible, whether an orbit of a two-dimensional map is chaotic or not. This new method is based on the frequency analysis of a data series constructed by recording the logarithm of the amplification factor of the deviation vector of nearby orbits. Accordingly, two datasets are recorded and the χ^2 -likelihood of their power spectra is computed. Ordered orbits have always the same power spectrum, so their $\chi^2 \equiv \psi^2$ acquires a zero value. On the contrary, a chaotic orbit has a power spectrum that varies with time, hence, chaotic orbits always exhibit a non-zero ψ^2 value. Even as regards "sticky" orbits, the PSI method is very effective in the early detection of chaos, while the global behavior of the ψ^2 indicator can provide information (also) on the intense of the chaotic behavior, i.e., on how "strong" or "weak" the associated chaos may be.

keywords: dynamics, chaos, chaotic orbits, detection of chaos.

Submitted to: *J. Phys. A: Math. Theor.*

1. Introduction

A major issue in studying non-integrable dynamical systems is the determination, as early as possible, of the orbits' (chaotic or not) nature. In the pioneering work of Hénon and Heiles (1964), when the related research was limited to two-dimensional (2D) systems, the study of the orbits' nature was performed by means of the surface of section (SoS). When research extended to more complex, three-dimensional (3D) systems (where the method of SoS cannot be applied), the problem was addressed in terms of the Lyapunov characteristic numbers - LCN (Benettin et al. 1976, Froeschlé 1984). The LCN method tracks the evolution of the deviation vector, \vec{d} , that connects the positions of two nearby orbits in phase-space at each time-step or, equivalently, at

each iteration. Unfortunately both methods have the same weakness: They cannot distinguish, early enough, a "sticky" chaotic orbit from an ordered one (see, e.g., Contopoulos & Voglis 1997).

Since then, several other methods have been proposed. Some of them, are based on the analysis of a time-series associated to the values of the generalized coordinates or functions of these coordinates, as the rotation number method (Contopoulos 1966), the frequency map analysis (Laskar et al. 1992, Laskar 1993) and the power spectrum of quasi-integrals analysis (Voyatzis & Ichtiaroglou 1992). Other methods, use the geodesic divergence of initially nearby trajectories, as in the probability-density analysis of stretching numbers (Froeschlé et al. 1993, Voglis & Contopoulos 1994), the fast Lyapunov indicators (Froeschlé et al. 1997), and the methods of alignment indexes, namely, the small alignment indexes - SALI (Skokos 2001, Skokos et al. 2003, 2004, Skokos & Manos 2016) and the generalized alignment indexes - GALI (Skokos et al. 2007, Skokos & Manos 2016). Each and everyone of the above methods has its own advantages and weaknesses; some of them are more efficient to addressing 2D systems rather than their higher-dimensional counterparts, while others perform better on mappings rather than flows.

In this context, eighteen years ago, Vozikis et al. (2000) proposed a method based on the frequency analysis (power spectrum) of stretching numbers. A variant of this method was used also by Karanis & Vozikis (2008). The method is fast and efficient, but it has a major disadvantage. In order to decide whether an orbit is regular or not, one needs to visually inspect the power spectrum and to classify it as either representing a regular orbit or a chaotic one.

In the present article, we are revisiting the method proposed by Vozikis et al. (2000), introducing a major improvement, that may help us to override the previous disadvantage. As a result of this new method, we end up with (just) a single number that enables us to classify an orbit as being either regular or chaotic.

This article is organized as follows: In Section 2, we summarize the power-spectrum method of Vozikis et al. (2000), in the context of which we will set up also our new model. In Section 3, we perform a *goodness-of-fit*, χ^2 -analysis of several successive power spectra, resulting from datasets that are associated with the deviation vectors of three particular types of orbit, namely, regular, chaotic, and "sticky". As a result of the aforementioned likelihood analysis, a new indicator of chaotic behavior is introduced (Section 4), which allows us to classify any kind of orbit on a 2D mapping, as early as possible. Finally, we conclude in Section 5.

2. The model and the power spectrum method

2.1. The model

One of the most frequently used test-models for studying chaotic motion is the 2D *standard map*, appearing in literature in too many forms (Lichtenberg & Leiberman

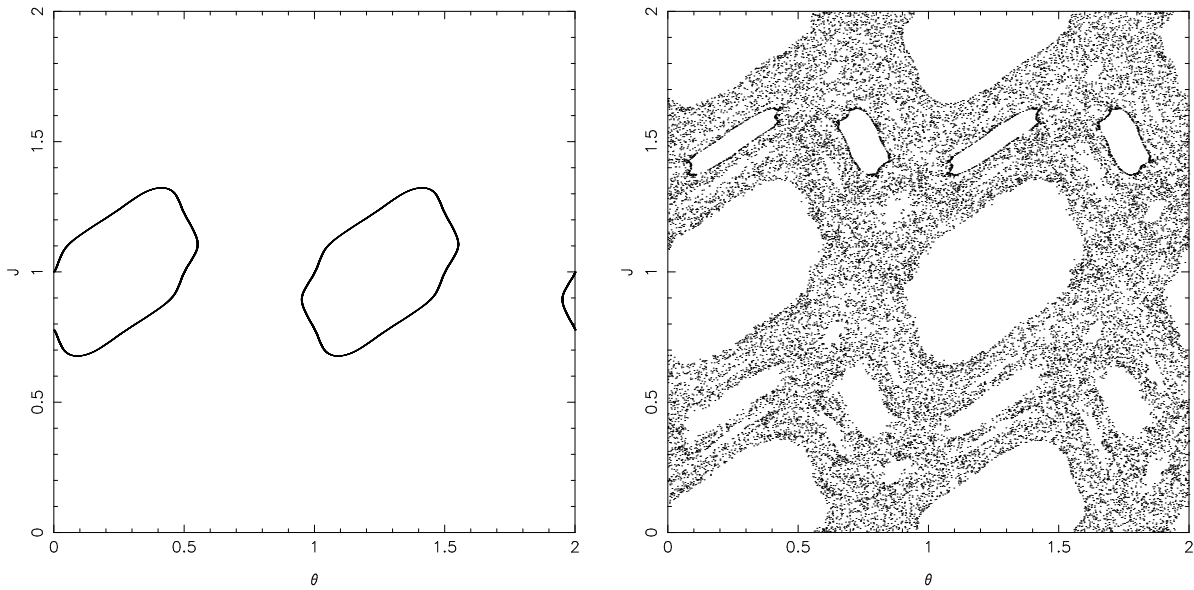


Figure 1. Successive points of two orbits on the *standard map*, when $k = 0.7$. Left frame, an ordered orbit originating at $J_0 = \pi$, $\theta_0 = 1.5 \pi$; Right frame, a chaotic orbit originating at $J_0 = 1.3 \pi$, $\theta_0 = 1.5 \pi$ (the axes units are in multiples of π).

1983, Ichikawa et al 1987, Aubry and Abramovici 1990, Contopoulos & Voglis 1997, Gelfreich 1999, Lazutkin 2005). In the present article, we adopt the following set of recursive relations

$$J_{i+1} = J_i + k \cos(2\theta_i) \quad \text{mod}(2\pi), \quad (1a)$$

$$\theta_{i+1} = \theta_i + J_{i+1} \quad \text{mod}(2\pi), \quad (1b)$$

where J_i and θ_i are the associated action-angle variables, i stands for the iteration number, and k is the "*stochasticity parameter*" (see, e.g., Lichtenberg & Lieberman 1983). In what follows, we consider that $k = 0.7$, a case where the standard map possess both regular and chaotic regions.

In figures 1, 2 and 3 we present four characteristic orbits of the standard map, for $k = 0.7$. Notice that, in all figures, J_i and θ_i are given as multiples of π . The two frames of figure 1 represent the first 20 000 points of an ordered orbit, with initial conditions $J_0 = \pi$, $\theta_0 = 1.5 \pi$ (left frame), and of a chaotic orbit, with initial position at $J_0 = 1.3 \pi$, $\theta_0 = 1.5 \pi$ (right frame). The left frame of figure 2 represents a chaotic orbit, originating at $J_0 = 1.1998 \pi$, $\theta_0 = 1.49 \pi$. Although the orbit looks ordered, a zoom (right frame) on the area near the separatrix reveals its chaotic nature. Finally the two frames of figure 3 represent a "*sticky*" orbit with initial position $J_0 = \pi$, $\theta_0 = 1.538 \pi$. The left frame shows the first 10 000 successive points, while the right one presents the corresponding 15 000 ones. This "*sticky*" orbit, although it is chaotic, behaves, at least macroscopically, like an ordered one for about 11 000 iterations.

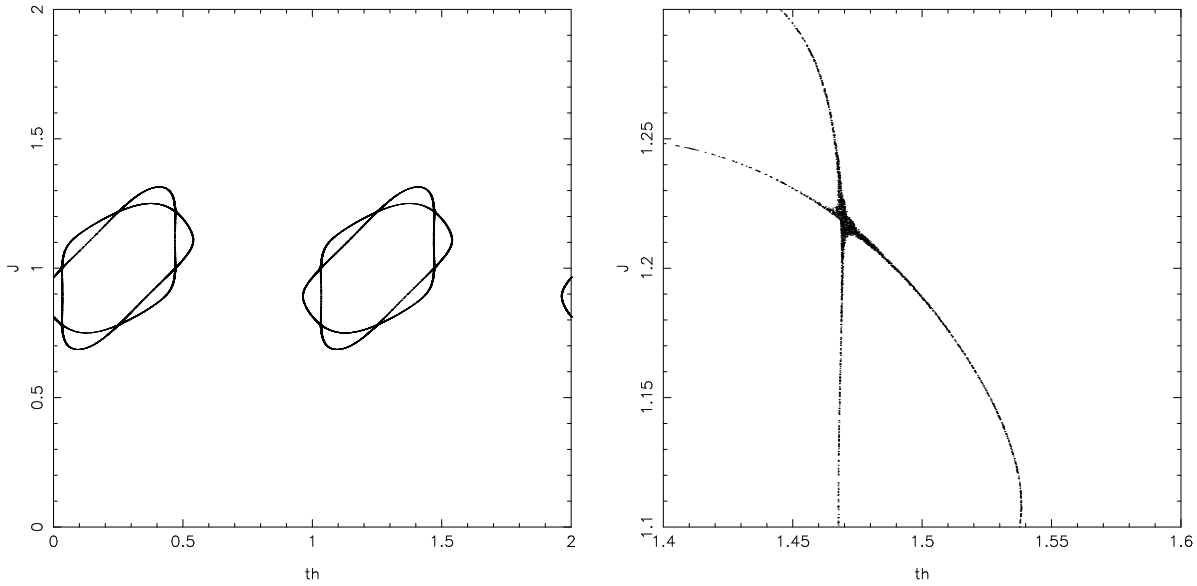


Figure 2. Successive points of a chaotic orbits on the *standard map*, when $k = 0.7$ originating at $J_0 = 1.1998 \pi$, $\theta_0 = 1.49 \pi$. Left frame, full view; Right frame, a zoom on the area near the separatrix of the orbit.

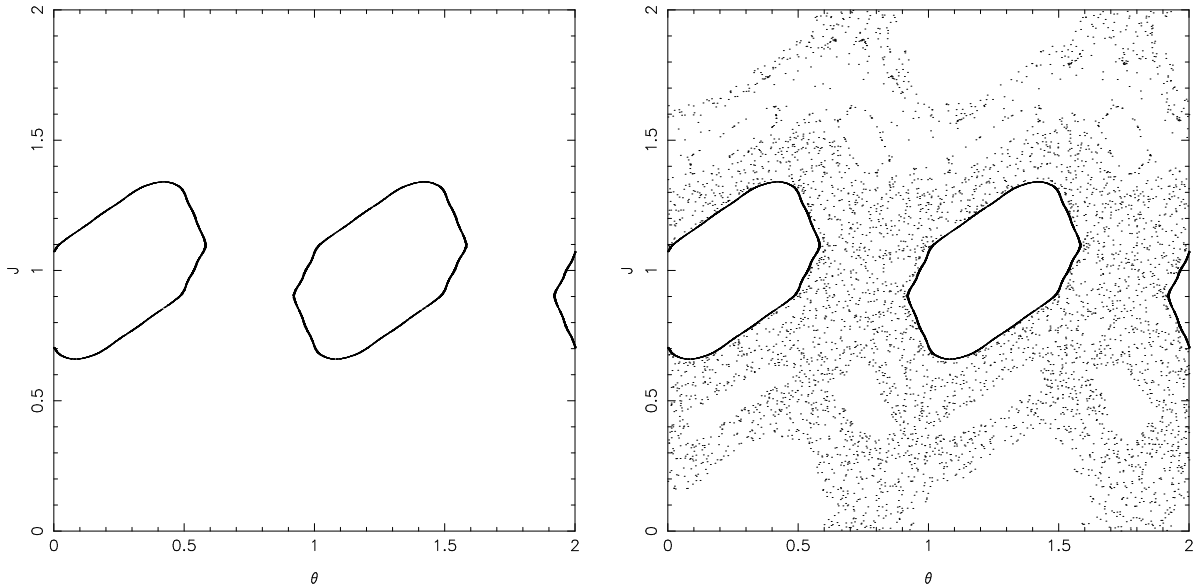


Figure 3. Successive points of a “sticky” orbit originating at $J_0 = \pi$, $\theta_0 = 1.538 \pi$. Left frame, the first 10 000 points; Right frame, the first 15 000 points.

2.2. The power spectrum (PSOD) method

In order to decide on the nature of an orbit (chaotic or not), Vozikis et al. (2000) proposed the Power Spectrum of Orbits Divergence (PSOD) method. This method consists in the numerical integration of the orbit originating at (J_0, θ_0) , along with a nearby one, originating at an infinitesimally-close distance in phase space, $\vec{d}_0 = (dJ_0, d\theta_0)$, i.e., of an initial position $J'_0 = J_0 + dJ_0$, $\theta'_0 = \theta_0 + d\theta_0$. At each iteration, i ,

the quantity

$$q_i = \ln(d_i/d_0) , \quad (2)$$

where $\vec{d}_i = (dJ_i, d\theta_i)$, is recorded. To calculate \vec{d}_i , instead of integrating numerically also the second, nearby, orbit, one can use the so called *variational equations*

$$\begin{aligned} dJ_{i+1} &= dJ_i - 2k \sin(2\theta_i) d\theta_i \\ d\theta_{i+1} &= d\theta_i + dJ_{i+1}. \end{aligned} \quad (3)$$

These equations can be easily obtained, by substituting in the standard map $J' = J + dJ$ and $\theta' = \theta + d\theta$, and expanding $\sin(2\theta')$ as a Taylor series, keeping only first order terms in dJ and $d\theta$. Prior to any iteration, the deviation vector, \vec{d} , is renormalized, upon multiplication by the factor d_0/d_i . In other words, at each and every i , although \vec{d}_i retains the orientation acquired, its norm remains equal to d_0 . Thus, after tracking this orbit for N successive iterations, we are left with a series of consecutive q_i ($i = 1, 2, \dots, N$).

The power spectrum of the aforementioned q -series can be obtained by taking the discrete Fourier transform of q_k , multiplied by a *window function*, w_k ,

$$Q_j = \sum_{k=0}^{2N-1} q_k w_k e^{2\pi i \frac{j}{N} k} \quad j = 0, \dots, (2N - 1) . \quad (4)$$

As window function we use the so-called *Hanning window* (see, e.g., Press et al. 1992). In this context, the power spectrum, $P(f_j)$, is defined over a set of $M = N + 1$ frequencies, f_j , as

$$\begin{aligned} P(f_0) &= \frac{1}{W} |Q_0|^2 , \\ P(f_j) &= \frac{1}{W} (|Q_j|^2 + |Q_{2N-j}|^2) \quad j = 1, \dots, (N - 1) , \\ P(f_c) &= \frac{1}{W} |Q_N|^2 , \end{aligned} \quad (5)$$

where we have set

$$W = 2N \sum_{k=0}^{2N-1} w_k^2 . \quad (6)$$

In Eqs. (5), the frequency $f_c = f_N$ is the Nyquist frequency, which, in the case of the standard map, is

$$f_c = \frac{1}{2}. \quad (7)$$

The group of frequencies embraced by the power spectrum of Eqs. (5), is given by:

$$f_j = f_c \frac{j}{M} \quad j = 0, \dots, M \quad (8)$$

More elaborated details on the calculation of the power spectrum can be found in the book "*Numerical Recipes*" by Press et al. (2001). In this article, as far as the computation of the power spectrum is concerned, we use two sets of successive $2 \times N$ data, which overlap with each other by one half of their lengths. In other words, the

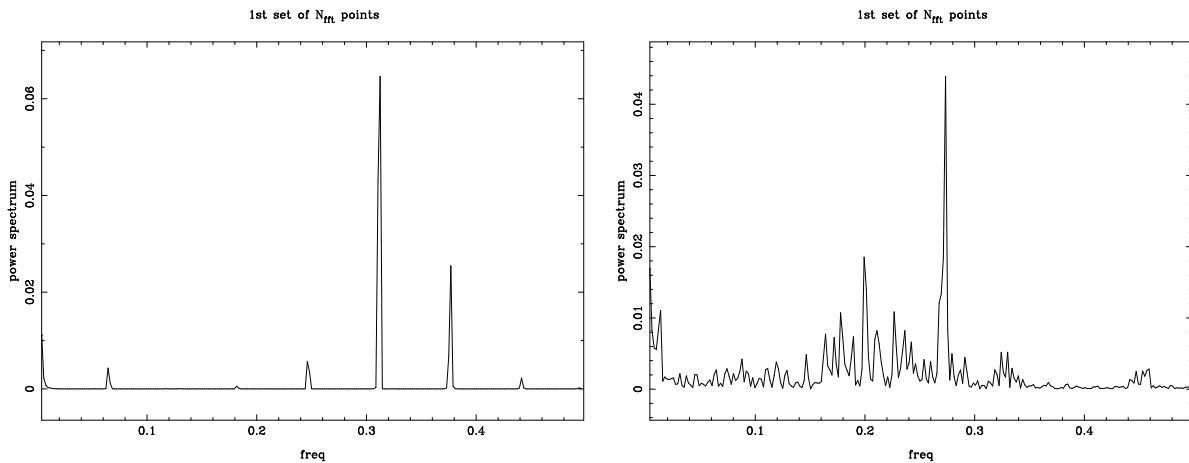


Figure 4. The power spectra of two orbits for $N_s = 3 \times 256$ iterations. Left frame: The power spectrum associated to the ordered orbit originating at $J_0 = \pi$, $\theta_0 = 1.5 \pi$. Right frame: The corresponding quantity as regards the chaotic orbit originating at $J_0 = 1.3\pi$, $\theta_0 = 1.5 \pi$.

whole dataset q_i involved in a single calculation of the power spectrum is $N_S = 3 \times N$, where N is a power of 2.

Figure 4 presents the power spectra associated with the two orbits of figure 1. The spectrum on the left frame is for the regular orbit, while the one on the right frame is for the chaotic. One may easily decide on the nature of a particular orbit, simply by inspecting its spectrum. Ordered motion corresponds to a power spectrum with only a few spikes in certain frequencies. On the contrary, a chaotic orbit exhibits a spectrum that consists of almost all frequencies, with varying amplitudes.

3. A novel method

3.1. The basic idea

The basic idea behind our new method is that, ordered motion is a kind of quasi-periodic motion. Thus, the power spectrum of an ordered orbit will always have some sort of characteristic frequencies, i.e., it will be independent of time (or, equivalently, of the iteration number). On the contrary, chaotic motion is a sort of random walk. Hence, we expect that for a chaotic orbit, two different sets of q_i (eq. 2) recorded on different times (iterations) will be completely different, since the motions possess no periodicity at all.

The validity of this idea can be easily inspected in figures 5 to 7. In all three figures, at first, we follow a specific orbit for $N_S = 3 \times 256$ iterations. The spectrum of the associated set of q_i is presented on the left frame of each figure. Next, we follow the same orbit for another N_S iterations, thus creating a second set of q_i . The spectrum of this second set is presented on the right frame. In figure 5, the two successive spectra of an ordered orbit are presented. These two spectra appear to be the same. On the contrary, as far as a chaotic orbit is concerned, the difference between the associated

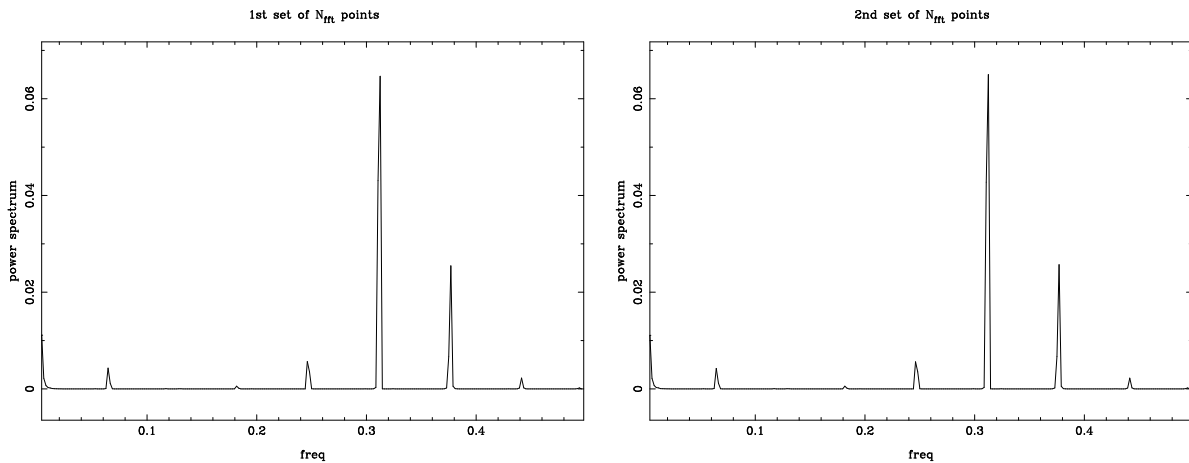


Figure 5. The PSODs of the first $N_S = 3 \times 256 = 768$ iterations (left) and the next N_S iterations (right) of an ordered orbit originating at $J_0 = \pi$, $\theta_0 = 1.5 \pi$.

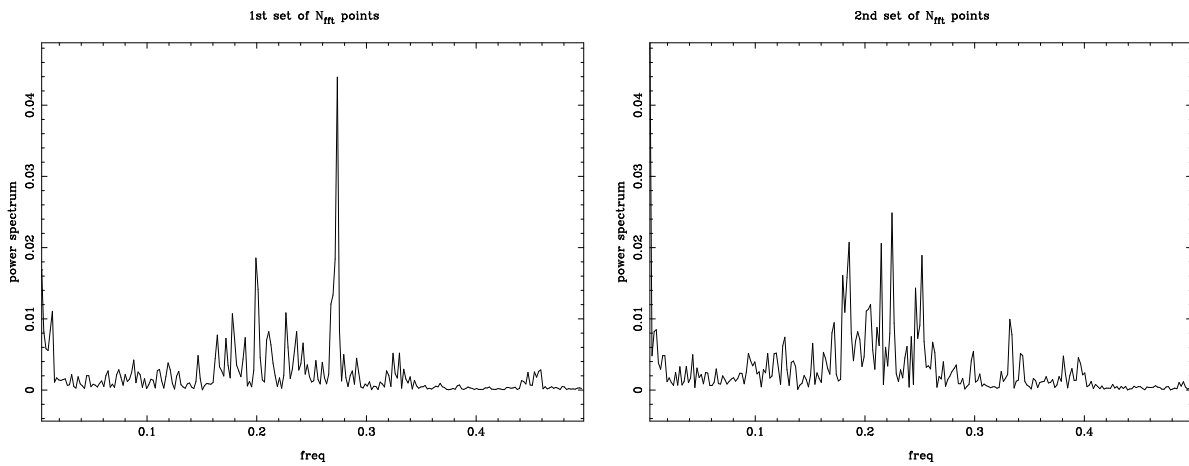


Figure 6. Same as figure 5, but, this time, for a chaotic orbit originating at $J_0 = 1.3 \pi$, $\theta_0 = 1.5 \pi$.

two spectra is more than obvious (cf. figure 6).

Detecting the chaotic nature of a "sticky" orbit is the most challenging case, since such an orbit can behave like an ordered one for many iterations. A reliable *chaos-detecting tool* must reveal the true identity of these orbits as early as possible. Figure 7 shows the two spectra of a "sticky" orbit. We see that these spectra resemble the ones of an ordered orbit. However, although they appear to be the same, upon a closer look we see that they are not: There are small differences at those frequencies that are associated to low amplitudes.

3.2. On the χ^2 -likelihood of the PSOD method

In order to see if and how much the PSOD of the same orbit changes we perform a χ^2 -statistics, as regards two PSODs of a particular orbit.

Let P_j be the power spectrum $P(f_j)$ of the first PSOD ($j = 1, 2, \dots, N_S$) and P'_j the corresponding spectrum, $P(f_{j'})$, of the second PSOD ($j' = N_S + 1, \dots, i$). Their χ^2

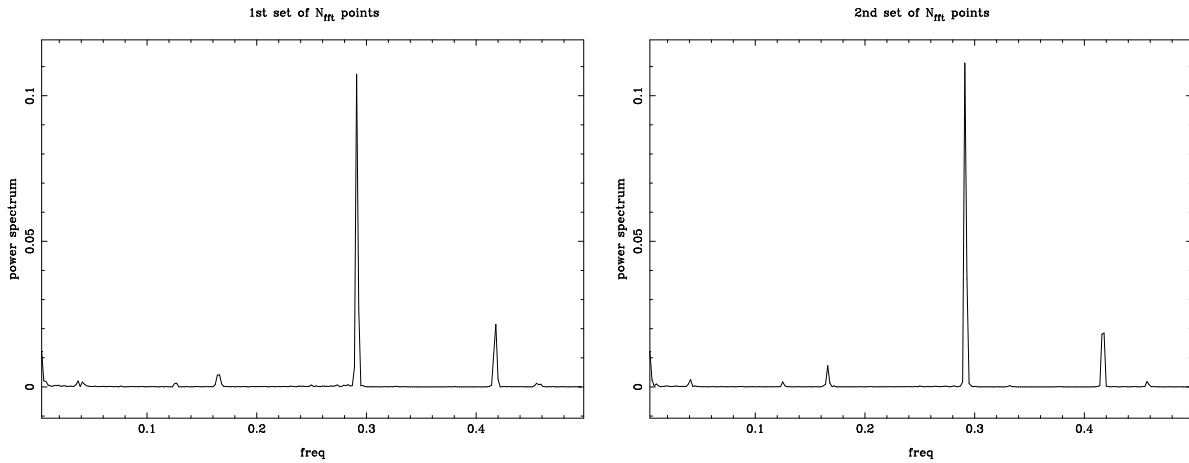


Figure 7. Same as figures 5 and 6, but now, as far as the "sticky" orbit originating at $J_0 = \pi$, $\theta_0 = 1.538 \pi$ is concerned.

likelihood is, then, defined as (see, e.g., Chapter 14.3 of Press et al. 1992)

$$\chi^2 = \sum_{j=0}^M \frac{(P'_j - P_j)^2}{P'_j + P_j}. \quad (9)$$

Since the values of P'_j of the second PSOD depend on the particular set of q_i , we consider that the second PSOD, P'_j , is a function of the iteration number i , namely,

$$\begin{aligned} P_j &= \text{PSOD} [q(1), \dots, q(N_S)] , \\ P'_j(i) &= \text{PSOD} [q(i - N_S + 1), \dots, q(i)] . \end{aligned} \quad (10)$$

As a consequence, now, χ^2 becomes also a function of the iteration number, i .

$$\chi^2 = \chi^2(i) = \sum_{j=0}^M \frac{(P'_j(i) - P_j)^2}{P'_j(i) + P_j}. \quad (11)$$

To begin with, let us examine how $\chi^2(i)$ behaves for various types of orbits (i.e., ordered, chaotic, or "sticky") and if the idea suggested in Section 3.1 is valid, in the sense that it can give us reliable results as far as the early prediction of chaos is concerned. Figure 8 shows the evolution of $\chi^2(i)$ of the PSODs as a function of the iteration number, i , for the four orbits of figures 1,2 and 3. The top left frame corresponds to the ordered orbit, having initial conditions $J_0 = \pi$, $\theta_0 = 1.5 \pi$. As we can see, the corresponding $\chi^2(i)$ value remains zero, for every i . As we have already discussed in Section 3.1, an ordered orbit represents a sort of quasi-periodic motion and, thus, its PSOD will exhibit only a few, characteristic frequencies, remaining time-invariant (or, equivalently, invariant with respect to the iteration number, i). On the contrary, chaotic orbits behave in a definitely non-periodic manner and, therefore, their PSOD will be completely different at different times (equivalently, at different values of the iteration number, i). The top right frame of figure 8 depicts the evolution of $\chi^2(i)$ for a chaotic orbit, originating at $J_0 = 1.3 \pi$, $\theta_0 = 1.5 \pi$. As we can see, in this case, $\chi^2(i)$ starts from a value of 0.23 and fluctuates, but it never gets a zero value. A similar behavior can be seen

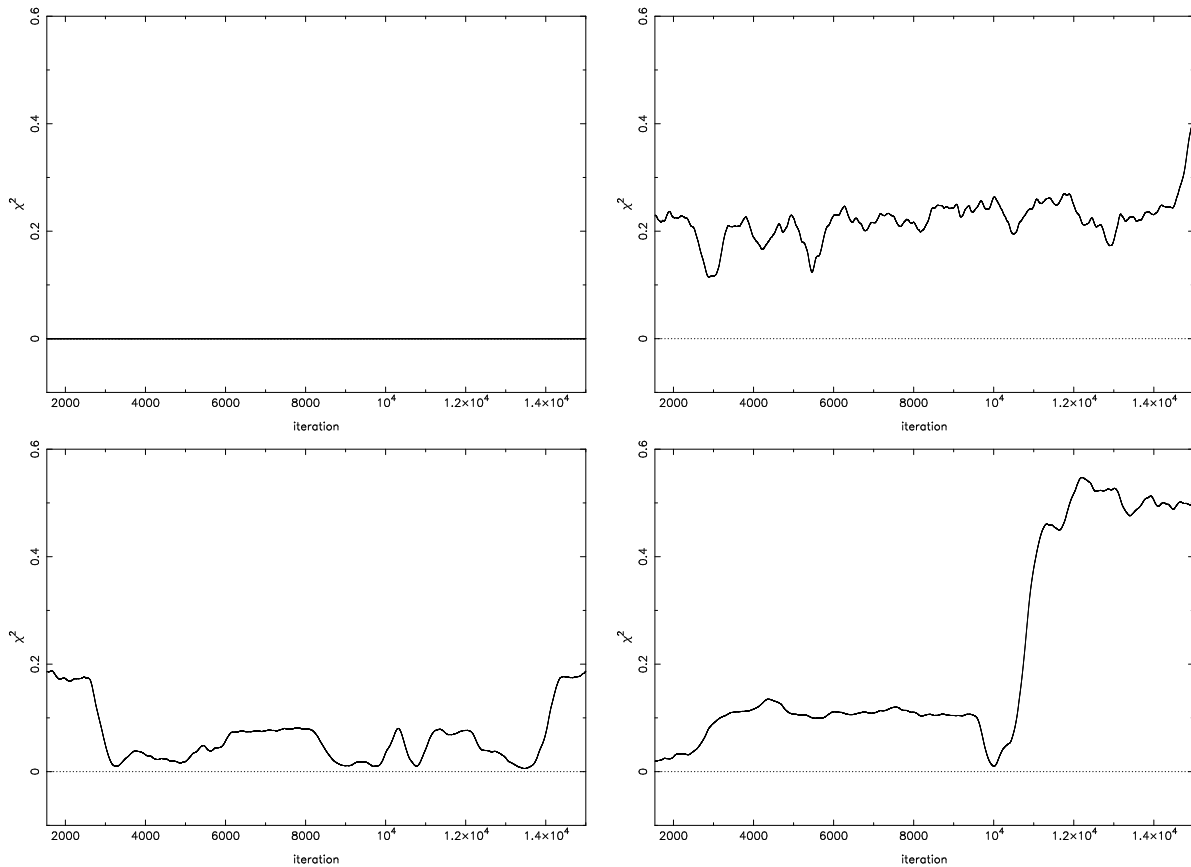


Figure 8. $\chi^2(i)$ -likelihood of the PSODs corresponding to the orbits of figure 1. Top left frame, the ordered orbit originating at $J_0 = \pi$, $\theta_0 = 1.5 \pi$; Top right frame, the chaotic orbit originating at $J_0 = 1.3 \pi$, $\theta_0 = 1.5 \pi$; Bottom left frame, the second chaotic orbit originating at $J_0 = 1.1998 \pi$, $\theta_0 = 1.49 \pi$; Bottom right frame, the "sticky" orbit originating at $J_0 = \pi$, $\theta_0 = 1.538 \pi$.

also in the evolution of $\chi^2(i)$ of the second chaotic orbit, originating at $J_0 = 1.1998 \pi$, $\theta_0 = 1.49 \pi$. This orbit, although it presents very weak chaos (cf. figure 2), exhibits, from the very beginning, a value of $\chi^2(i)$ around 0.18. The final, bottom right frame of figure 8 represents the evolution of $\chi^2(i)$ associated to the "sticky" orbit, originating at $J_0 = \pi$, $\theta_0 = 1.538 \pi$. We can see that, even in the beginning, where it is not easy at all to (visually) distinguish the difference between the two PSODs (cf. figure 7), the $\chi^2(i)$ method can reveal the true nature of the orbit, acquiring a value of 0.03. To put it more clearly, in this case, the non-zero value of $\chi^2(i)$ of the two PSODs indicates that there are differences between them and, therefore, in the end, the orbit will exhibit a clearly chaotic behavior. Indeed, as the time (or, equivalently, the iteration number, i) goes by, $\chi^2(i)$ increases and, when the particular orbit leaves the "sticky" region and enters into the "big chaotic sea", it climbs to values higher than 0.5!

4. The power spectrum indicator, ψ^2

So far, we have seen that, as regards two PSODs of a particular orbit, the $\chi^2(i)$ -likelihood analysis can give us important information on whether this orbit is ordered or not. Clearly, a non zero value of χ^2 suggests that the orbit is definitely chaotic. In this context, the results of Section 3.2 may give rise to the following questions:

- (i) Why does the χ^2 value corresponding to the "sticky" orbit rises to such high values, as compared to the chaotic orbits presented in figure 8?
- (ii) Can we modify the method, in a way that it can give us (also) a clear indication on the degree of chaos?

The answer to the first question is easy. The two spectra we compare for the χ^2 -analysis, differ significantly, not only on the frequencies but also on the total power,

$$S_P(i) = \sum_{j=0}^M P_j(i)', \quad (12)$$

of each spectrum. The orbit migrates from a region of weak (i.e., not visually observable) chaos to a region with strong chaotic behavior. Figure 9 shows the evolution of the total power spectra, $S_P(i)$, corresponding to the four orbits associated with the $\chi^2(i)$ values of figure 8.

In an effort to answer the second question, we (further) ask ourselves: "What our results would be, if we compared two power spectra yielded from datasets that differ only a few (i.e., a constant number, n , of) iterations apart?"

To do so, instead of taking the first data set as corresponding to the beginning of the orbit, i.e., to originate from $i = 1$, we consider that it ends at the iteration $i - n$. In this case, the (two) power spectra corresponding to the iteration i are

$$\begin{aligned} P_j'(i) &= \text{PSOD} [q(i - N_S + 1), \dots, q(i)] \\ P_j(i) &= \text{PSOD} [q(i - N_S + 1 - n), \dots, q(i - n)] \end{aligned} \quad (13)$$

and their χ^2 likelihood, which is our new Power Spectrum Indicator (PSI), to be (from now on) denoted by ψ^2 , is given by

$$\psi^2(i) \equiv \sum_{j=0}^M \frac{(P_j'(i) - P_j(i))^2}{P_j'(i) + P_j(i)} = \chi^2(i). \quad (14)$$

Figure 10 presents the evolution of our new indicator, ψ^2 , as a function of the iteration number i , regarding the four orbits of figure 1. The two spectra are calculated from datasets that are $n = 256$ iterations apart. As expected, for the ordered orbit (upper left frame) the value of ψ^2 is always zero. On the contrary, the two chaotic orbits (upper right and lower left) exhibit a clearly non-zero value of ψ^2 . This value is by no means constant, because, at different values of the iteration number, i , the orbit visits different areas of the chaotic region. Notice that, the values of ψ^2 corresponding to the first chaotic orbit (upper right frame), are much higher than those of the second

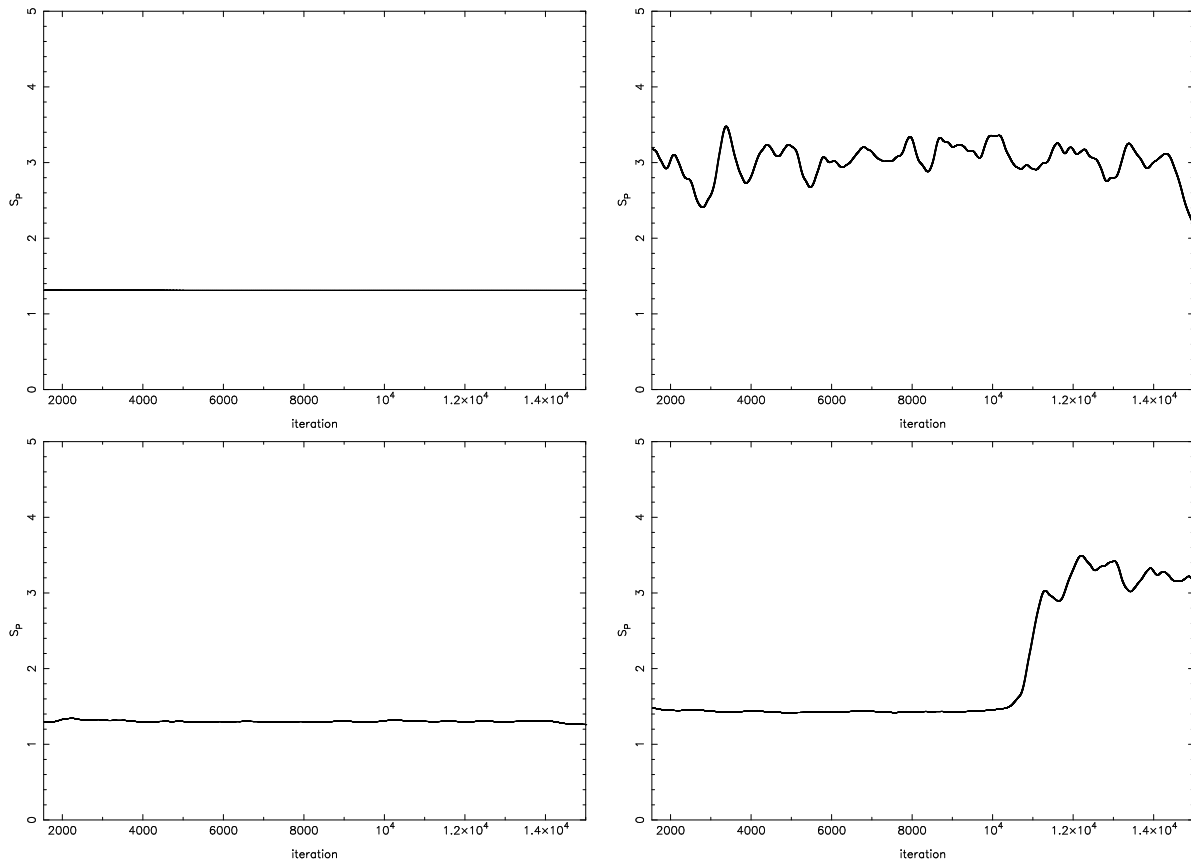


Figure 9. The evolution of the total power, $S_P(i)$, of the spectra associated to the four orbits of figure 8.

one (lower left frame), indicating that the former orbit is in a region of *“strong”* chaos, as compared to the *“weaker”* chaotic region in which the latter orbit lies up.

Finally, as regards the power spectrum indicator, ψ^2 , associated with the *“sticky”* orbit (lower right frame of figure 10), it initially admits a low, but clearly non-zero value, indicating that it rests in a *“weak”* chaotic region. However, after a lot of iterations, the orbit migrates from the *“weak”* chaotic region to a region with *“stronger chaos”*, analogous to the region of the first chaotic orbit. Accordingly, the value of ψ^2 climbs to higher levels, exhibiting a behavior similar to that of the first chaotic orbit.

At this point, we need to stress that, the potential values of ψ^2 depend on the separation n of the two datasets. The lower the value of n , the closer the two datasets are, hence, their ψ^2 will be lower. Note that for $n < N_s$ the two datasets have $N_s - n$ common data. Nevertheless, even for $n = 64$ ($N_s = 3 \times 256$) the PSI method gives quite accurate results, as it can be readily seen from figure 11.

As mentioned above, the value of $\psi^2(i)$ give us a local (i.e., in the region currently visited by the orbit) indication of how strong the chaos may be. In order to attain a global indicator (i.e., one that will cover the whole area visited by an orbit), we should

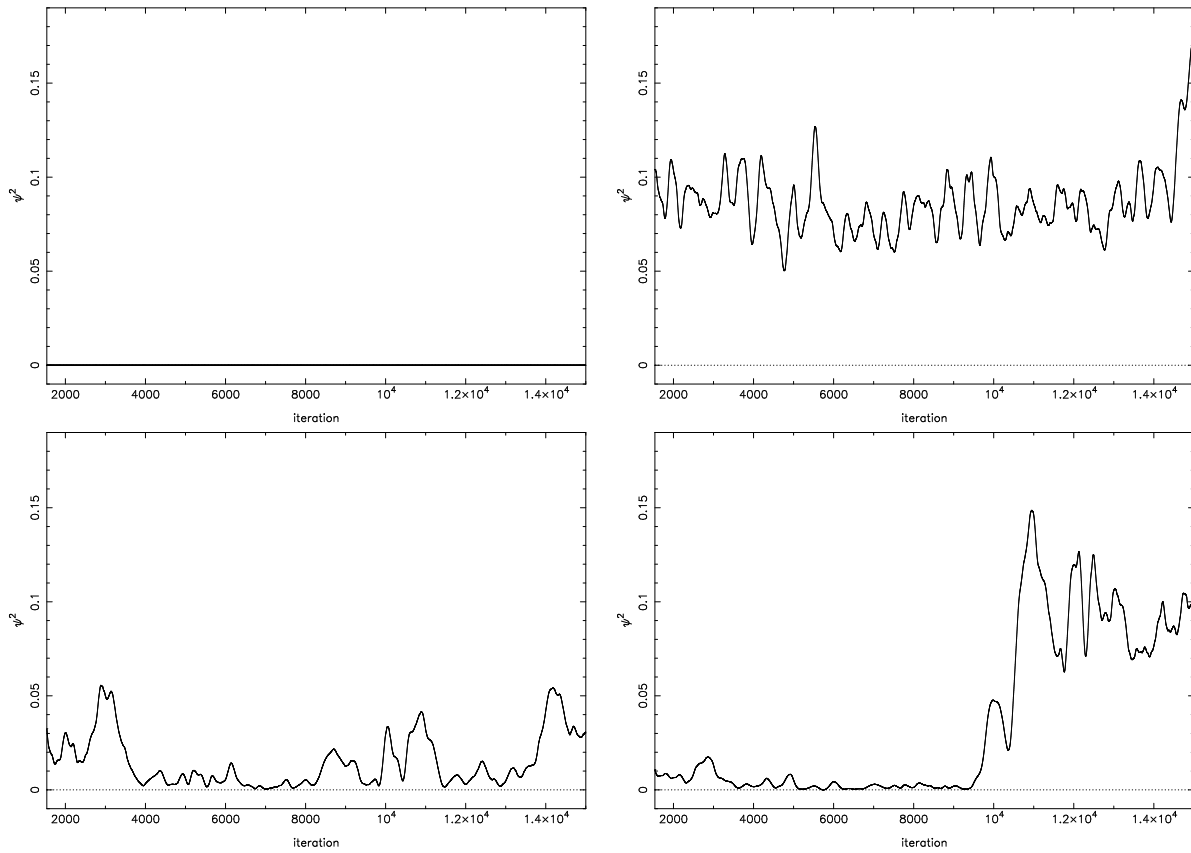


Figure 10. The evolution of $\psi^2(i)$ associated to the four orbits depicted in figure 1. The top left frame corresponds to the ordered orbit, originating at $J_0 = \pi$, $\theta_0 = 1.5 \pi$. Top right: The first chaotic orbit, originating at $J_0 = 1.3 \pi$, $\theta_0 = 1.5 \pi$. Bottom left: The second chaotic orbit, originating at $J_0 = 1.1998 \pi$, $\theta_0 = 1.49 \pi$. Bottom right: The power spectrum indicator associated to the "sticky" orbit, originating at $J_0 = \pi$, $\theta_0 = 1.538 \pi$. In each and every one of these cases, the datasets involved differ with each other by $n = 256$ iterations.

consider the average value of ψ^2 , defined as

$$\langle \psi^2 \rangle (i) = \frac{1}{i - N_s - n + 1} \sum_{j=N_s+n}^i \psi^2(j). \quad (15)$$

Figure 12 shows the evolution of $\langle \psi^2 \rangle$ for the four orbits considered throughout this article. Their ψ^2 indicators are computed upon the use of a dataset separation of $n = 256$ iterations.

5. Conclusions

In the present paper we propose a new tool, to be called Power Spectrum Indicator (PSI), or ψ^2 , that enables us to determine, as early as possible, the chaotic nature of orbits in dynamical systems. This new method is based on the method of Vozikis et al. (2000), i.e., on the frequency analysis of a data series constructed by recording the logarithm of

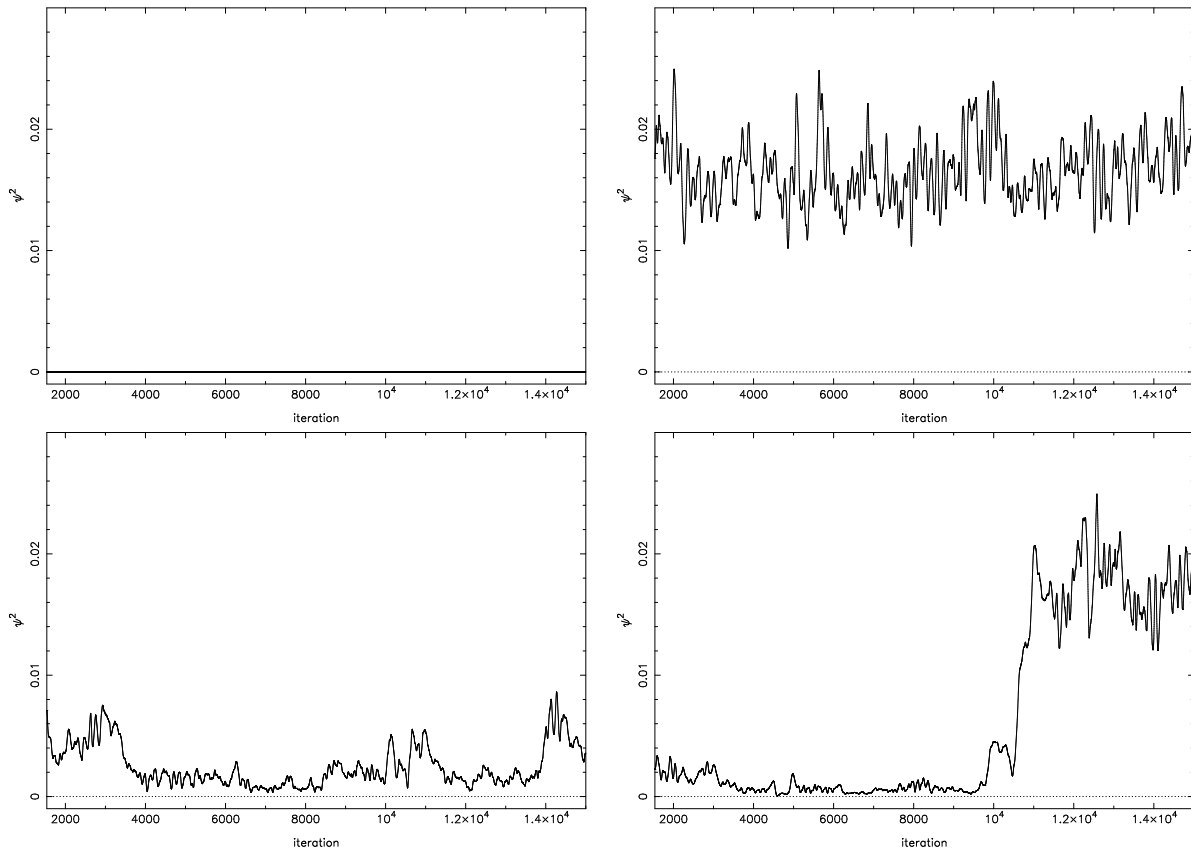


Figure 11. Same as figure 10, but for $n = 64$.

the amplification factor of the deviation vector of nearby orbits. For this reason, two datasets are recorded and the χ^2 -likelihood of their power spectra is computed.

Ordered orbits have always the same power spectrum, so their $\psi^2 \equiv \chi^2$ acquires an ever-zero value. On the contrary, a chaotic orbit has a power spectrum that varies with time (equivalently, with the number of iterations). Therefore, chaotic orbits always exhibit a non-zero ψ^2 value, hence, by calculating the ψ^2 of an orbit, we can easily decide if this is chaotic or not. Even for "sticky" orbits, the PSI method is very effective in the early detection of chaos. Eventually, the global behavior of the ψ^2 indicator can provide information (also) on the intense of the chaotic behavior, i.e., on how "strong" or "weak" the associated chaos may be.

However, we need to stress that, the aforementioned results refer to the case where the system under study is a 2D mapping. Further investigation is needed, if the ψ^2 method is to be implemented also in Hamiltonian flows. As stated in the discussion of Vozikis et al. (2000), the difference between maps and flows is that, in the case of flows, a detailed analysis concerning the selection of the renormalization time is needed, since it may significantly affect the corresponding results.

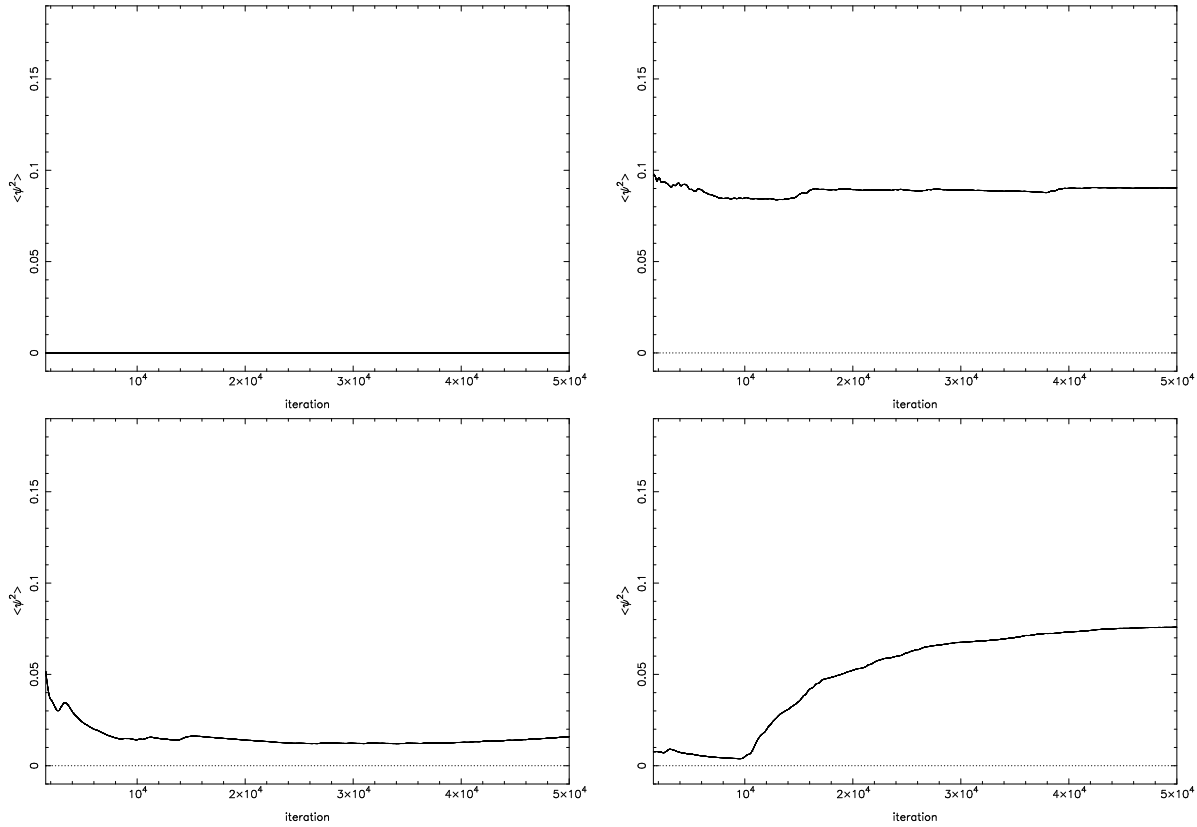


Figure 12. The evolution of the global indicator $\langle \psi^2 \rangle(i)$, for $n = 256$, as regards the four orbits presented in figure 1. Top left, the ordered orbit originating at $J_0 = \pi$, $\theta_0 = 1.5 \pi$; Top right, the chaotic orbit originating at $J_0 = 1.3 \pi$, $\theta_0 = 1.5 \pi$; Bottom left, the second chaotic orbit originating at $J_0 = 1.1998 \pi$, $\theta_0 = 1.49 \pi$; Bottom right, the "sticky" orbit originating at $J_0 = \pi$, $\theta_0 = 1.538 \pi$.

Acknowledgments

Financial support by the Research Committee of the Technological Education Institute of Central Macedonia at Serres, Greece, under grant SAT/CE/201217-aa/01, is gratefully acknowledged.

References

- Aubry S and Abramovici G 1990 *Physica D* **43** 199
 Benettin G, Galgani L and Strelcyn J M 1976 *Phys. Rev. A* **14** 2338
 Contopoulos G 1966 *Les Nouvelles Méthodes de la Dynamique Stellaire* ed F Nahon and M Hénon (Paris: CNRS)
 Contopoulos G and Voglis N 1997 *Astron. Astroph.* **317** 73
 Hénon M and Heiles C 1964 *AJ* **69** 73
 Froeschlé C, 1984 *Cel. Mech.* **34** 95
 Froeschlé C, Froeschlé Ch and Lohinger E 1993 *Cel. Mech. Dyn. Astron.* **51** 135
 Froeschlé C, Lega E and Gonzi R 1997, *Cel. Mech. Dyn. Astron.* **67** 41
 Gelfreich V G 1999 *Commun. Math. Phys.* **201** 155
 Ichikawa Y H, Kamimura T and Hatori T 1987 *Physica D* **29** 247

- Karanis G and Vozikis Ch 2008 *Astron. Nachr.* **320** 403
- Laskar J 1993 *Physica D* **67** 257
- Laskar J, Froeschlé C and Celletti A 1992 *Physica D* **56** 253
- Lazutkin V F 2005 *J. Math. Science* **128** 2687
- Lichtenberg A J and Leiberman M A 1983 *Regular and stochastic motion* (New York: Springer) pp. 77-84)
- Press W H, Teukolsky S A, Vetterling W T and Flannery B P 1992 *Numerical Recipes in Fortran – The Art of Scientific Computing 2nd edn* (Cambridge: Cambridge University Press)
- Skokos Ch 2001 *J. Phys. A: Math. Gen.* **34** 10029
- Skokos Ch, Antonopoulos C, Bountis A and Vrahatis M N 2003 *Prog. Theor. Phys. Suppl.* **150** 439
- Skokos Ch, Antonopoulos C, Bountis A and Vrahatis M N 2004 *J. Phys. A: Math. Gen.* **37** 6269
- Skokos Ch, Bountis A and Antonopoulos C G 2007 *Physica D* **231** 30
- Skokos Ch and Manos T 2016 *Chaos Detection and Predictability (Lecture Notes in Physics vol 915)* ed Skokos Ch, Gottwald G and Laskar J (Berlin, Heidelberg : Springer)
- Voglis N and Contopoulos G 1994, *J. Phys. A: Math. Gen.* **27** 4899
- Voyatzis G and Ichtiaroglou S 1992 *J. Phys. A: Math. Gen.* **25** 5931
- Vozikis Ch L, Varvoglis H and Tsiganis K 2000 *Astron. Astrophys.* **359** 386